Journal of
Nuclear Engineering

MDPI

Article

Structure-Dependent Doppler Broadening Using a Generalized Thermal Scattering Law

Nina C. Fleming * and Ayman I. Hawari

Department of Nuclear Engineering, North Carolina State University, Raleigh, NC 27695, USA; aihawari@ncsu.edu
* Correspondence: ncsorrel@ncsu.edu

Abstract: The thermal scattering law (TSL), i.e., $S(\alpha,\beta)$, represents the momentum and energy exchange phase space for a material. The incoherent and coherent components of the TSL correlate an atom's trajectory with itself and/or with other atoms in the lattice structure. This structural information is especially important for low energies where the wavelength of neutrons is on the order of the lattice interatomic spacing. Both thermal neutron scattering as well as low energy resonance broadening involve processes where incoming neutron responses are lattice dependent. Traditionally, Doppler broadening for absorption resonances approximates these interactions by assuming a Maxwell–Boltzmann distribution for the neutron velocity. For high energies and high temperatures, this approximation is reasonable. However, for low temperatures or low energies, the lattice structure binding effects will influence the velocity distribution. Using the TSL to determine the Doppler broadening directly introduces the material structure into the calculation to most accurately capture the momentum and energy space. Typically, the TSL is derived assuming cubic lattice symmetry. This approximation collapses the directional lattice information, including the polarization vectors and associated energies, into an energy-dependent function called the density of states. The cubic approximation, while valid for highly symmetric and uniformly bonded materials, is insufficient to capture the true structure. In this work, generalized formulation for the exact, lattice-dependent TSL is implemented within the Full Law Analysis Scattering System Hub (*FLASSH*) using polarization vectors and associated energies as fundamental input. These capabilities are utilized to perform the generalized structure Doppler broadening analysis for UO_2.

Keywords: cross sections; Doppler broadening; thermal scattering law; *FLASSH*

Citation: Fleming, N.C.; Hawari, A.I. Structure-Dependent Doppler Broadening Using a Generalized Thermal Scattering Law. *J. Nucl. Eng.* **2021**, *2*, 124–131. https://doi.org/10.3390/jne2020013

Academic Editor: Luka Snoj

Received: 1 October 2020
Accepted: 27 March 2021
Published: 8 April 2021

1. Introduction

The neutronics of a nuclear reactor are defined by cross sections which represent the possible modes of interaction. In the resonance region, the effects of the neutron–nucleus interaction have been approximated using free gas models in our reactor codes for many years. These approximations assume a Maxwellian velocity distribution to perform the Doppler broadening of resonance cross sections. At high temperatures or in weakly bound systems, this approximation reasonably represents a solid system. However, implicit in this approximation is the neglection of lattice effects, resulting in a shift in the peak energy and changes to the line shape. These lattice effects are especially significant at lower temperatures and in more tightly bound systems.

Doppler broadening correlates the change in temperature with variations in the available momentum and energy states of the lattice which result in changes to the cross section. The possible modes of energy and momentum exchange for a material are inherent material properties defined by the thermal scattering law (TSL), i.e., $S(\alpha,\beta)$, which can be also defined as $S(\vec{\kappa},\omega)$, or the dynamic structure factor. The TSL holds the structure information for a material, and it has been previously calculated in the NJOY and *FLASSH* (Full Law Analysis Scattering System Hub) codes and used for thermal scattering cross

section evaluations [1,2]. The TSL historically applied to thermal scattering cross sections also defines the structure-dependent Doppler broadening of cross section resonances.

Historically, the TSL was calculated under the cubic approximation which assumes isotropic forces in the material unit cell. This approximation reduces the structure information found in the polarization vectors and associated frequencies to the density of states which represents the cubic, directionally averaged frequency space. Codes such as NJOY and SAMMY use this cubic approximated *S(α,β)* in their calculations [1,3]. However, the cubic approximation ignores the directional dependencies of the structure. For many materials this approximation is valid. However, for non-cubic materials such as those with differing bond types or those with non-ideal structures, the cubic formulation is insufficient. In this work, a generalized formulation for the TSL was implemented within the *FLASSH* code and used to calculate the *S(α,β)* for UO_2. The generalized *S(α,β)* was used in performing generalized Doppler broadening to determine a structure-dependent broadened cross section which is compared here with experimental cross sections.

2. Generalized Thermal Scattering Law

The thermal scattering law is fundamentally split into two parts: the self scattering law (*Ss*) and the distinct scattering law (S_d) [4],

$$S\left(\vec{\kappa},\omega\right) = S_s\left(\vec{\kappa},\omega\right) + S_d\left(\vec{\kappa},\omega\right) \tag{1}$$

where S is a function of $\vec{\kappa}$ and ω, the scattering vector and frequency, respectively. The self component correlates the atomic motion of an atom relative to itself. The distinct component compares the atom's movement with the entire structure. Under the incoherent approximation, the thermal scattering law only consists of the self component and the distinct component is assumed to be negligible. As temperature increases, the motion of the atoms within the lattice will increase, impacting the magnitude of the TSL.

2.1. Generalized Formulation of the TSL

The generalized formulation for the self scattering law is defined as

$$S_s^m\left(\vec{\kappa},\omega\right) = \frac{1}{2\pi\hbar}\int_{-\infty}^{\infty} \exp[i\omega t]\exp\left[Q_m\left(\gamma_m(\vec{\kappa},t) - \gamma_m(\vec{\kappa},0)\right)\right]dt \tag{2}$$

where the self component is calculated for distinct atoms m [5]. Furthermore, the exponential components are defined as

$$\gamma_m(\vec{\kappa},t) = \frac{1}{N}\sum_s \left[\coth\left(\frac{\hbar\omega_s}{2k_BT}\right)\frac{\cos(\omega_s t)}{\omega_s} + i\frac{\sin(\omega_s t)}{\omega_s}\right]\left|\vec{e}_\kappa\cdot\vec{e}_{s,m}\right|^2 \tag{3}$$

$$\gamma_m(\vec{\kappa},0) = \frac{1}{N}\sum_s \frac{1}{\omega_s}\coth\left(\frac{\hbar\omega_s}{2k_BT}\right)\left|\vec{e}_\kappa\cdot\vec{e}_{s,m}\right|^2, \text{ and} \tag{4}$$

$$Q_m = \frac{\hbar\kappa^2}{2M_m} \tag{5}$$

where N is the number of wave vectors sampled in the first Brillouin zone, k_B is the Boltzmann constant, t is time, and M_m is the mass [5]. The material information is found in the frequency (ω_s) and polarization vector ($\vec{e_s}$) variables. These are indexed with a subscript s indicating the correspondence of the particular wave vector and polarization index. The scattering vector $\vec{\kappa}$ is divided into its magnitude and unit vector $\vec{e_\kappa}$. Under the cubic approximation, the scattering vector is reduced such that the directionalized dot product $\left|\vec{\kappa}\cdot\vec{e_s}\right|^2$ reduces to $k^2/3$. In this work, the exact dot product and polarization information is maintained in order to preserve the material structure information. These

equations defining the TSL are identical to those used in the thermal scattering cross section evaluation.

2.2. Implementation of the General Forumulation into FLASSH

The generalized TSL formulation given in Equations (2)–(5) was included into the generalized incoherent TSL evaluation in *FLASSH*. The phonon expansion of the equations above results in a Taylor series expansion to facilitate implementation into the code as described in Reference [6]. These equations were implemented using OpenMP to allow for parallelized computing. Additionally, *FLASSH* has options for automatic α/β gridding to capture the structure and features of the TSL. The generalized formulation requires the polarization vectors and associated frequencies as input. This information can be predictively calculated from ab initio simulations in codes such as VASP and PHONON [7–9].

3. Structure-Dependent Doppler Broadening

As temperature changes, the thermal motion of the atoms within the lattice will result in a broadening of cross section resonances seen in the Doppler broadening process. Doppler broadening, most generally, is captured by the convolution of the cross section with the appropriate distribution function. Historically, a Maxwellian velocity distribution was used to correlate the resonance peak broadening to temperature. The free gas approximation results in a symmetrical Gaussian broadening of the resonance peak. This approximation ignores the lattice binding effects and assumes a free gas probability distribution. Under this free gas approximation, the Doppler broadened cross section is equal to

$$\sigma(E) = \frac{\sigma_0 \Gamma^2}{4} \int_0^\infty dE_n \ \frac{S^{FG}(E_n, E)}{(E_n - E_0)^2 + (\Gamma/2)^2} \tag{6}$$

where S^{FG} is the energy distribution resulting from the Maxwellian velocity distribution, σ_0 is the peak value of the resonance cross section, Γ is the total resonance width, E_0 is the resonance energy (lab frame), E is the kinetic energy of the incident neutron (lab frame), and E_n is the energy of the incident neutron relative to the target nucleus [10]. Expanding the distribution in the numerator, the cross section is defined explicitly under the free gas approximation as

$$\sigma(E) = \frac{\sigma_0 \Gamma^2}{4} \frac{1}{\sqrt{\pi}\Delta} \sqrt{\frac{E_0}{E}} \int_0^\infty dE_n \ \frac{\exp\left[\frac{-(E_n - E_0)^2}{\Delta^2}\right]}{(E_n - E_0)^2 + (\Gamma/2)^2}, \qquad \Delta = 2\sqrt{\frac{m}{M} k_B T E} \tag{7}$$

where m is the mass of the neutron, M is the mass of the target, k_B is the Boltzmann constant, and T is the temperature [10].

Similarly, an exact derivation of Doppler broadening for a bound system would implement a velocity distribution specific to the material rather than approximate it with the Maxwellian velocity distribution. The velocity distribution (or more accurately the energy and momentum distribution) for a specific material is defined by the TSL. The resulting Doppler broadened cross section using the TSL rather than the Maxwellian distribution is equal to

$$\sigma(E) = \frac{\sigma_0 \Gamma^2}{4} \int_{-\infty}^\infty d\beta \ \frac{e^{-\beta/2} S(\alpha, \beta)}{(E - E_0 - \beta k_B T)^2 + (\Gamma/2)^2} \tag{8}$$

where $S(\alpha,\beta)$ is the scattering law, α is dimensionless momentum transfer, and β is dimensionless energy [10]. In order to represent the structure of the material, the binding effects introduced in the scattering law are needed. However, in the limit as energy and temperature increase, the scattering law distribution will approach that of the free gas, and

therefore, the lattice impacts to Doppler broadening are most important for low energy resonances.

Common practice in most nuclear data codes has been to performed Doppler broadening using Equation (7) under the free gas approximation [1,3]. Implementing the generalized TSL evaluation from *FLASSH* into the Doppler broadening operation introduces the structure information and removes all symmetry approximations, accurately capturing the structure impacts in Doppler broadening.

4. Results

The generalized TSL routine was tested for UO_2 and implemented into the Doppler broadening routine. As a common fuel material, UO_2 and its Doppler broadened cross section have significant applications in reactor physics and criticality safety. UO_2 was modeled with ab initio lattice dynamics in the VASP and PHONON codes [7–9]. This model was used to generate the ENDF/B-VIII thermal scattering libraries for UO_2 and represents an ideal crystal matrix for UO_2 [11,12]. Using the GGA-PBE pseudopotential with an added Hubbard model to represent the coulomb repulsion for the *5f* electrons, a 2 × 2× 2 supercell was utilized to determine the Hellman–Feynman forces within the system (unit cell displayed in Figure 1) [12].

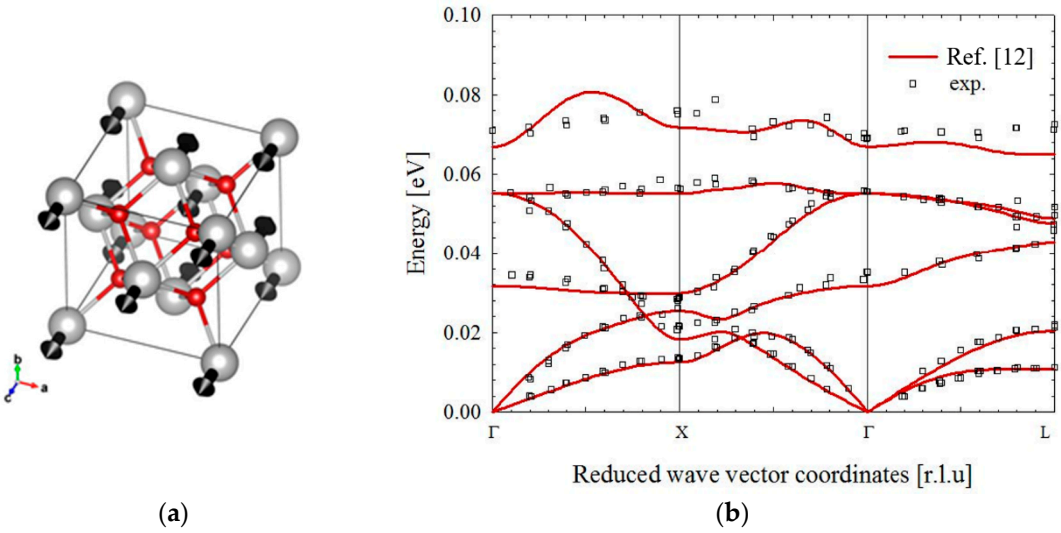

Figure 1. (**a**) UO_2 unit cell. The unit cell to the left has black arrows demonstrating the *5f* magnetic moments. Oxygen atoms are shown in red and uranium atoms are shown in grey (Data from Ref. [12]). (**b**) UO_2 dispersion relations. The calculated values for the dispersion relations shown on the right are compared with experimental data [12–14].

The Hellman–Feynman forces were calculated with a 600 eV plane wave cutoff and 3 × 3 × 3 k-mesh. These forces were then used in the PHONON code to sample the phonon dispersion relations for 8 million wave vectors, corresponding to 24 million polarization vectors and frequencies for a single unit cell. The dispersion relations for UO_2 calculated by this model are compared with experimental data in Figure 1 [12].

The polarization data corresponding to the dispersion relations shown in Figure 1 were used as input into *FLASSH* to calculate the generalized scattering law using Equations (2)–(5). Using the free atom cross section of 9.29938 barns for uranium, a phonon order of 100, and a mass of 238.0508 amu for uranium, the $S(\alpha,\beta)$ for uranium in UO_2 was calculated at 23.7 K. This lower temperature emphasizes the lattice impact for better comparison with experimental data. The α-grid was calculated to directly correspond with the energy grid for the resonance cross section, and the β-gridding was constructed automatically within *FLASSH* based on the energy resolution of the inputs.

The degree of non-cubicity of a material is demonstrated in the Debye–Waller matrix. For a cubic material, the main diagonal elements will be equivalent, with zero or nearly zero

off-diagonal terms. The Debye–Waller matrix for UO_2, given in Table 1 below, demonstrates the cubic behavior of UO_2.

Table 1. Debye–Waller matrix for UO_2 at 23.7 K.

	X	Y	Z
X	7.05×10^{-4}	5.39×10^{-7}	5.39×10^{-7}
Y	5.39×10^{-7}	7.05×10^{-4}	5.39×10^{-7}
Z	5.39×10^{-7}	5.39×10^{-7}	7.05×10^{-4}

The generalized $S(\alpha,\beta)$ was evaluated and compared with the cubic evaluation as shown below in Figure 2. In general, the cubic and generalized treatments show reasonable agreement as expected. As a function of α, few deviations are seen between the two methods. For low lying resonances on the order of a few eV, α values around 1 to 5 are the most significant. From β equals zero to approximately β equals 0.3, the TSL is smooth. This low β region will have the highest impact on cross section evaluations. Therefore, the slight increase in the generalized TSL seen at lower β for the generalized method will propagate into the Doppler evaluation. Maximum differences in the evaluations are seen as a function of β, with the highest impact seen at points corresponding to the peaks in the TSL. Examples of this can be seen around β-values of 0.35 and 0.8 where the deviations fluctuate significantly from positive to negative. Both the generalized and the cubic methods capture the same peaks in the TSL; however, the resolution of the generalized peaks is more precise. At higher β, most of the deviations are numerical combined with decaying peaks as seen in the fluctuation from positive to negative differences. The value of the TSL as β increases becomes very small and approximately negligible with regards to the cross section evaluation.

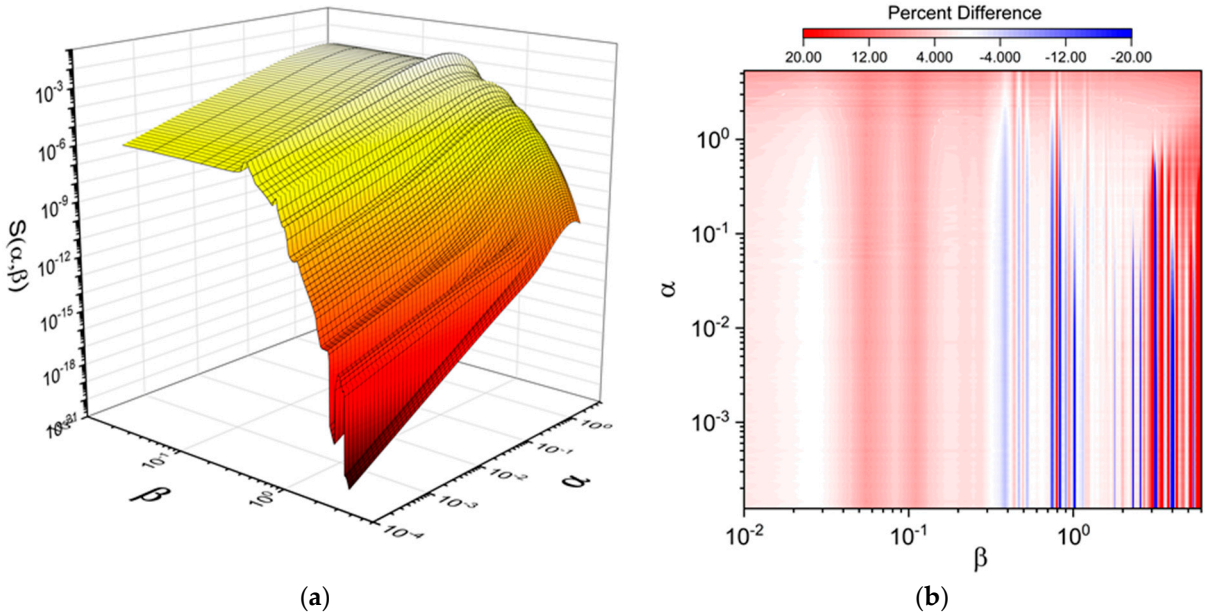

Figure 2. (**a**) Generalized UO_2 $S(\alpha,\beta)$ as a function of both α and β. (**b**) The percent difference between the generalized and cubic evaluations are displayed.

The TSL evaluation was also verified using moment checks. When both α and $\vec{e_\kappa}$ are held constant, the TSL takes the form of a Gaussian function of β [15]. The definition of $S(\alpha,\beta)$ then dictates that

$$\int_{-\infty}^{\infty} S(\alpha,\beta)\, d\beta \;\; = 1 \tag{9}$$

and

$$\int_{-\infty}^{\infty} \beta\, S(\alpha,\beta)\, d\beta \;\; = -\alpha \tag{10}$$

which correspond to the 0th and 1st moments, respectively. For the generalized TSL, the 0th and 1st moments were both evaluated to be 1.016 for α-values in the Doppler range. These deviations from unity seen for the generalized TSL could potentially be the result of the many random directions sampled in the calculation (i.e., $\vec{e_\kappa}$ is not held constant). The variation from unity also implies that the function deviates from Gaussian. Given the cubic structure of UO_2, this behavior of the moments for the generalized treatment is reasonable and highlights the correspondence of the generalized and exact treatments for UO_2.

The generalized TSL was then used to Doppler broaden the lowest energy resonance for UO_2. In order to perform the Doppler broadening, a modified version of the SAMMY 8.1.0 code was used [3]. Modifications to the code allowed for a general *S(α,β)* to be input into the crystal lattice module Doppler broadening routine already present within the code. Using inputs from *FLASSH* in SAMMY, a free gas, generalized lattice, and cubic lattice Doppler broadening were performed. For the free gas calculation, effective temperatures were calculated using the density of states from the UO_2 ENDF/B-VIII model [16]. For a temperature of 23.7 K, the effective temperature is 91.07 K [16]. As expected, given the low temperature, the deviation between the actual and effective temperatures is large due to the more distinct lattice effects. The resulting Doppler broadened cross sections for the 6.67 eV resonance for UO_2 are displayed in Figure 3 for a temperature of 23.7 K.

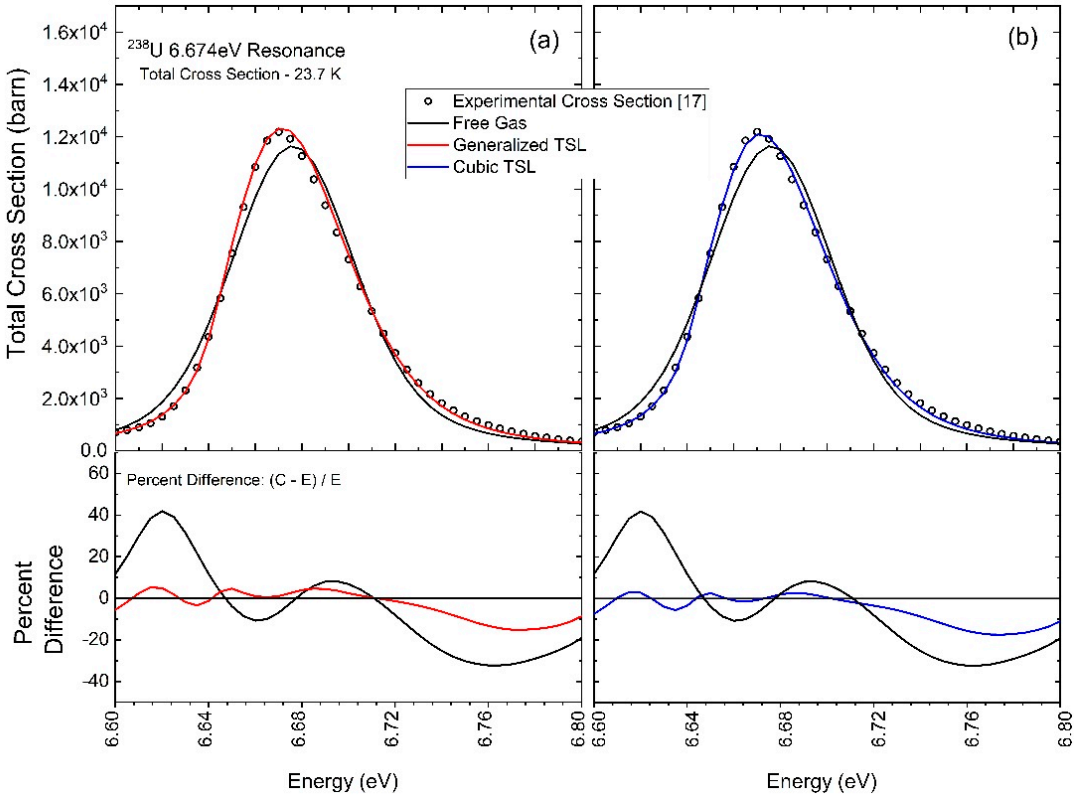

Figure 3. UO_2 Doppler broadened cross sections at 23.7 K. The cross section evaluation is compared with experimental data [17]. The generalized TSL was used for Doppler broadening in (**a**) and the cubic TSL in (**b**).

In Figure 3, the structure impacts on Doppler broadening can be clearly seen in the experimental data. With the lower temperature and the low energy resonance, the asymmetry of the peak and deviation from Gaussian behavior are clearly seen. The free gas approximation is unable to capture this effect with deviations up to 41% from

the experiment at 23.7 K. However, using the lattice model, the Doppler broadening accurately shifts the resonance peak and broadens the data with maximum deviations of 15% and 17% for the generalized and cubic cases, respectively. The differences between the generalized and cubic treatments highlighted in the TSL and moments can be seen in the small changes to the broadened curves. As a nearly cubic material, however, the two TSLs consistently Doppler broadened the resonance peak. With this implementation, the generalized structure can be accurately represented in $S(\alpha,\beta)$ calculations with compatible evaluation of temperature impacts through the Doppler broadening region.

5. Conclusions

A generalized TSL evaluation was implemented in the *FLASSH* code. This generalized evaluation captures the structure information of the target material and provides the necessary probability distribution for accurate Doppler broadening. A structure-dependent Doppler broadening based on the generalized *FLASSH* TSL was implemented and tested for UO_2. The TSL derived under the generalized formulation showed reasonable agreement with the cubic evaluation, and the differences due to the generalized structure were noted in the variation to the Doppler broadening. These generalized results improved the evaluation to have a maximum deviation of 15% at 23.7 K. The evaluations were conducted for the ideal UO_2 crystal structure system. However, the methods implemented will allow for analysis of any structure with potentially high impacts for materials with non-cubicity, e.g., due to high exposure. Furthermore, with the methods set in place, the thermal scattering cross section and the Doppler broadening operation both utilize the same TSL for consistent cross section evaluation.

Author Contributions: N.C.F.: Formal analysis, software, methodology, visualization, validation, and writing—original draft preparation; A.I.H.: conceptualization, methodology, validation, writing—review and editing, supervision, and funding acquisition. All authors have read and agreed to the published version of the manuscript.

Funding: This work was partially funded by the US National Nuclear Security Administration's (NNSA) Nuclear Criticality Safety Program (NCSP), the US Naval Nuclear Propulsion Program (NNPP), and the US Department of Energy's Nuclear Energy University Program (NEUP).

Institutional Review Board Statement: Not applicable.

Informed Consent Statement: Not applicable.

Conflicts of Interest: The authors declare no conflict of interest. The funders had no role in the design of the study; in the collection, analyses, or interpretation of data; in the writing of the manuscript, or in the decision to publish the results.

References

1. MacFarelane, R.E.; Muir, D.W.; Boicourt, R.M.; Kahler, A.C., III; Conlin, J.L. *The NJOY Nuclear Data Processing System Version 2016*; LA-UR-17-20093; Los Alamos National Laboratory: Los Alamos, NM, USA, 2016.
2. Zhu, Y.; Hawari, A.I. Full Law Analysis Scattering System Hub (*FLASSH*). In Proceedings of the PHYSOR 2018: Reactor Physics Paving the Way towards More Efficient Systems, Cancun, Mexico, 22–26 April 2018; pp. 966–976.
3. Larson, N.M. *Updated Users' Guide for SAMMY: Multilevel R-Matrix Fits to Neutron Data using Bayes' Equations*; ORNL/TM-9179/R8; Oak Ridge National Laboratory: Oak Ridge, TN, USA, 2008.
4. Hawari, A.I. Modern Techniques for inelastic thermal neutron scattering analysis. *Nucl. Data Sheets* **2014**, *118*, 172–175. [CrossRef]
5. Sjolander, A. Multi-phonon processes in slow neutron scattering by crystals. *Arkiv Fysik* **1958**, *14*, 315–371.
6. Sorrell, N.C.; Hawari, A.I. Development of a Generalized Lattice Symmetry Formulation for Thermal Scattering Law Analysis. In Proceedings of the ICNC 2019: 11th International Conference on Nuclear Criticality, Paris, France, 15–20 September 2019.
7. Kresse, G.; Furthmüller, J. Efficiency of ab-initio total energy calculations for metals and semiconductors using a plane-wave basis set. *Comput. Mater. Sci* **1996**, *6*, 15–50. [CrossRef]
8. Kresse, G.; Furthmüller, J. Efficient iterative schemes for ab initio total energy calculations using a plane-wave basis set. *Phys. Rev. B* **1996**, *54*, 11169–11186. [CrossRef] [PubMed]
9. Parlinski, K.; Li, Z.Q.; Kawazoe, Y. First-principles determination of the soft modes in cubic ZrO_2. *Phys. Rev. Lett.* **1997**, *78*, 4063–4066. [CrossRef]

10. Bernabei, A. The Effects of Crystalline Binding on the Doppler Broadening of a Neutron Resonance. Ph.D. Thesis, New York University, New York, NY, USA, 1964.
11. Brown, D.A.; Chadwick, M.B.; Capote, R.; Kahler, A.C.; Trkov, A.; Herman, M.W.; Sonzogni, A.A.; Danon, Y.; Carlson, A.D.; Dunn, M. ENDF/B-VIII.0: The 8th major release of the nuclear reactor data library with CIELO-project cross sections, new standards and thermal scattering data. *Nucl. Data Sheets* **2018**, *148*, 1–142. [CrossRef]
12. Wormald, J.L.; Fleming, N.C.; Hawari, A.I.; Zerkle, M.L. Generation of the thermal scattering law of uranium dioxide with ab initio lattice dynamics to capture crystal binding effects on neutron interactions. *Nucl. Sci. Eng.* **2021**, *195*, 227–238. [CrossRef]
13. Pang, J.W.L.; Chernatynskiy, A.; Larson, B.C.; Buyers, W.J.L.; Abernathy, D.L.; McClellan, K.J.; Phillpot, S.R. Phonon density of states and anharmonicity of UO_2. *Phys. Rev. B* **2014**, *89*, 115132. [CrossRef]
14. Dolling, G.; Cowley, R.A.; Woods, A.D.B. The crystal dynamics of uranium dioxide. *Can. J. Phys.* **1965**, *43*, 1397–1413. [CrossRef]
15. Squires, G.L. Correlation Functions in Nuclear Scattering. In *Introduction to the Theory of Thermal Neutron Scattering*; Cambridge University Press: Cambridge, UK, 2012.
16. Sorrell, N.C.; Hawari, A.I. Impact of the dynamic structure factor on Doppler broadening for ^{238}U in UO_2. *Trans. Am. Nucl. Soc.* **2018**, *119*, 720–723.
17. Meister, A.; Tagziria, H.; Royer, A.; Weigmann, H.; Bürkholz, C.; Van der Vorst, C. *Measurements to Investigate the Doppler Broadening of ^{238}U Neutron Resonances*; GE/R/ND/01/96; IRMM Reports: Geel, Belgium, 1996.